

DOI: 10.1002/aenm.201100719

Article type: Full Paper**Building on Soft Foundations – New Possibilities for Controlling Hybrid Photovoltaic Architectures***Joseph B. Franklin, Jonathan M. Downing, Finn Giuliani, Mary P. Ryan
and Martyn A. McLachlan**J. B. Franklin¹, J. M. Downing¹, F. Giuliani², M. P. Ryan³ and M. A. McLachlan¹¹Department of Materials and Centre for Plastic Electronics, Imperial College London, London SW7 2AZ, United Kingdom²Department of Materials and Department of Mechanical Engineering, Imperial College London, London SW7 2AZ, United Kingdom³Department of Materials and London Centre for Nanotechnology, Imperial College London, London SW7 2AZ, United KingdomE-mail: martyn.mclachlan@imperial.ac.uk

Keywords: Zinc Oxide, Conjugated Polymers, Organic Electronics, Thin Films, Hybrid Materials

Abstract

Here we outline a methodology for the deposition of a highly crystalline transparent conductive metal oxide (ZnO) onto a functionalised organic thin film poly (3-hexylthiophene, P3HT) without degradation of the microstructural, optical or electronic properties of the organic layer. To confirm the absence of damage we have assembled a simple bilayer photovoltaic (PV) device. The processing methodology has enabled us to demonstrate hybrid photovoltaic (h-PV) device formation in the conventional architecture for the first time. The compatibility of this novel low temperature processing route with π -conjugated molecular materials has tremendous potential for applications including electron accepting layers and optical spacers in organic PVs and light emitting diodes, as transparent electrodes and all future devices reliant on flexible substrates.

Introduction

Hybrid photovoltaic (h-PV) devices combine the favourable processing and absorption characteristics of π -conjugated molecular materials with the stability and electrical properties of inorganic materials.^[1] In particular, the combination of a wide band-gap metal oxide *e.g.* ZnO or TiO₂ with a conjugated polymer presents a pairing of materials suitable for the production of scalable, stable, nanostructured and ultimately more efficient photovoltaic devices. Despite this promise, h-PVs have yet to be prepared with efficiencies approaching even modest organic photovoltaics (OPVs). Attempts to address this challenge have mostly focused on morphological and microstructural control of the active layer.^[2-4] At present, h-PV devices are prepared either by *i)* deposition of the organic phase into a pre-grown metal-oxide layer,^[5, 6] or *ii)* co-deposition of both the inorganic and organic species.^[4] The deposition of highly crystalline metal-oxide *directly* on to any π -conjugated functional material, whilst maintaining the inherent integrity and properties of the organic layer, has yet to be demonstrated - primarily due to the elevated deposition or annealing temperatures of vacuum based processes or the requirements for substrate conductivity or harsh chemical conditions for solution-based processing methods.

For PV devices two distinct architectures may be prepared, namely the *conventional*^[17] and the so-called *inverted*^[18] structures. The conventional geometry requires first the deposition of the organic component onto the transparent electrode, typically indium tin oxide (ITO) coated glass, followed by the deposition of the organic material and metallic electrode. The preparation of the conventional configuration is more desirable as the transparent and metallic electrodes act as hole and electron acceptors respectively. Additionally, there is no contact between the metallic electrode and the organic material – thus avoiding unwanted reactions at this interface which have been shown to have a significant contribution to cell degradation.^[19]

^{20]} However the processing conditions used currently for oxide deposition mean that the inverted architecture has been the only reported h-PV structure thus far.

The necessity for developing techniques that allow metal oxides to be deposited onto functional organic materials extend far beyond h-PVs. For example, in the development of transparent conductive oxides (TCOs) on flexible substrates, optical spacers in solar cells^[7, 8] and LEDs,^[9-11] electron accepting layers in OPV devices^[12, 13] and multilayer devices.^[14] Here we demonstrate the use of pulsed laser deposition (PLD) as a method for depositing highly crystalline ZnO at low temperatures (200 °C) *directly* on to an functional organic thin film, poly(3-hexylthiophene) (P3HT). Importantly the oxide deposition conditions identified preserve the optical and electronic properties of the P3HT. This versatile and well-studied deposition technique allows precise control of the oxide film thickness, orientation and stoichiometry.^[15] Whilst PLD of indium tin oxide (ITO) has been previously demonstrated on flexible substrates^[16] we believe that this is the first demonstration of direct oxide deposition onto a functional organic material - and to the best of our knowledge the creation of the first conventional architecture h-PV device. The development of a reproducible methodology for preparing conventional architecture h-PV paves the pathway to effective studies into processing-performance relationships in h-PVs.

Thin Film Characterization

The X-ray diffraction (XRD) pattern of a ZnO film deposited on a 40 nm film of P3HT at 200°C (background of 50 mtorr O₂) on an ITO coated glass substrate is shown in **Figure 1a**. A highly crystalline film with a preferential (002) orientation is deposited *i.e.* the c-axis of the unit cell is aligned perpendicular to the substrate. In addition to the ZnO (002) family of diffraction peaks, ITO substrate peaks are observed at lower intensity. The inset (figure 1b) shows in detail the region of the ZnO (002) diffraction peak measured from films deposited

under different oxygen pressures. At 50 mtorr the measured full width at half-maximum (FWHM) of the (002) diffraction peak is $0.40^\circ 2\theta$, the peak position of $34.53^\circ 2\theta$ is close to that of a measured single crystal $34.55^\circ 2\theta$. A reduction in background oxygen pressure (< 50 mtorr) shifts the (002) diffraction peak to lower 2θ values, accompanied by an increase in the measured FWHM and a reduction in the peak area. In contrast, as the oxygen pressure is increased (> 50 mtorr) there is no systematic shift of the (002) diffraction peak or the measured FWHM however there is a reduction in the peak area.

Figure 1

Table 1

Background oxygen is necessary in PLD of ZnO to compensate for the zinc-rich species ejected from the target,^[21] additionally collisions with molecular oxygen in the chamber reduce the velocity of the ejected species arriving at the substrate. Therefore at low background oxygen pressure the ejected species will have minimal interaction with O_2 and will arrive at the substrate with a large amount of kinetic energy, which facilitates reorganisation at the substrate resulting in improved crystallinity.^[15] The observed shift in the (002) diffraction peak position is attributed to the formation of oxygen deficient films, at ~ 50 mtorr O_2 stoichiometry is achieved^[15] with no further shifts in peak position with increasing molecular oxygen content. The reduced peak intensity for films deposited at background oxygen pressures of 100 and 250 mtorr is attributed to two factors, firstly the reduced film thickness (Table 1) and secondly reduced crystallinity owing to interaction of the ejected species with molecular oxygen.

Film Morphology

Figures 2a-c show how ZnO film morphology changes with variation in oxygen pressure.

The films deposited at < 50 mtorr (Fig. 2a) typically show characteristic surface undulations which are attributed to the deformation of the underlying P3HT thin film, caused by the high energy incident particles. Increasing the oxygen pressure to 250 mtorr results in macroscopic crack formation in the films (Fig. 2b). The defect formation energy for oxygen interstitials (O_i) and zinc vacancies (V_{Zn}) is reduced as oxygen pressure increases.^[22] Although here we do not characterize such defects we speculate that at the highest oxygen pressure investigated (250 mtorr) the film defect density is increased, causing accumulation of strain leading to cracking. The slight shift in the (002) diffraction peak at 250 mtorr to a lower 2θ value is also indicative of the presence of strain in the film. At a background oxygen pressure of 50 mtorr a continuous, flat ZnO film is deposited across the entire substrate (12 x 12 mm) - the observed grain size of around 30 nm (Fig. 2c) is consistent with XRD measurements (Table 1).

A transmission electron microscope (TEM) cross-section of a multilayer device containing a ZnO layer deposited at 50 mtorr is shown in Figure 2d. Each layer in the device can be clearly observed and is labelled for clarity. Importantly the interface between the P3HT and the ZnO is extremely sharp and no ZnO is observed to have damaged or penetrated the underlying P3HT layer (Fig. 2e). The columnar morphology of ZnO film is clearly visible, which is anticipated owing to the preferential (002) orientation.^[23]

Figure 2

Optical Measurements and PV Device Characteristics

Figure 3a shows the optical transmission spectra of a pristine P3HT film and P3HT/ZnO multilayer films prepared as conventional and inverted device architectures. The sharp ZnO absorption at around 370 nm (~ 3.25 eV), is observed in all ZnO films prepared at all oxygen pressures. The broader absorption bands between 450 and 650 nm are attributed to π - π^*

transitions in the P3HT, the small shoulder at around 625 nm is indicative of inter and intra chain ordering.^[24] These are observed on all of the structures prepared and with no absorption quenching^[25] confirming our structural observation that the PLD of ZnO does not damage the P3HT. The UV-Vis data and TEM images confirm that no microstructural damage has occurred to the P3HT during the ZnO deposition.

Figure 3

The current-voltage (J-V) characteristics under dark and illumination of a conventional architecture device (ITO/40nm P3HT/150nm ZnO, 200 °C (50 mtorr)) are shown in figure 3b. The measured short circuit current (J_{sc}), open circuit voltage (V_{oc}), and fill factor were 0.18 mAcm^{-2} , 0.18 V, and 0.3 respectively. The calculated power conversion efficiency (PCE) was 0.01%. This modest performance is comparable to inverse ITO/ZnO/P3HT devices reported previously.^[5, 26] Here the remarkably flat interface between the P3HT and ZnO (Fig 2d-e), is likely to contribute significantly to the low PCE by minimising the interfacial area between polymer and oxide*. Device improvements could be achieved through interfacial roughening, optimization of layer thickness, electrode choice and processing conditions. However, the preparation of a conventional architecture h-PV device for the first time represents a significant and necessary step in h-PV development, and the methodology is applicable for a wider range of optoelectronic devices.

Conclusions

We have demonstrated for the first time the deposition of highly crystalline ZnO onto an organic functionalized substrate (P3HT) using pulsed laser deposition (PLD). By tuning the background oxygen pressure in the PLD chamber a deposition regime has been identified in which stoichiometric ZnO can be deposited without degradation or damage to the P3HT. At

* Planar ITO/P3HT/Ag and ITO/ZnO/Ag structures were prepared and their J-V measured under dark and AM 1.5 illumination. In both cases no photocurrent was detected with only diode behavior observed.

low oxygen pressure, (5 mtorr), the ZnO deposited is oxygen deficient and physical damage to underlying P3HT is observed owing to the high particle energy impacting on the *soft* P3HT. At high oxygen pressure (> 100 mtorr) the deposited films show extended cracks and surface defects. At 50 mtorr flat, continuous and stoichiometric ZnO layers can be deposited with no induced changes in the microstructure, optical or electronic properties of the P3HT. We have shown, for the first time that conventional architecture h-PV devices can be successfully prepared and predict improvements in device performance through modifications of the layer structure and cell configuration. The methodology presented represents an important step in comparing the device performance and photophysical processes in conventional and inverted architecture h-PV devices. More importantly, the wider requirement for transparent conducting oxides *i.e.* as optical spacers in multilayer devices, transparent top-electrodes various device technologies can be achieved using this methodology.

Experimental Section

P3HT deposition: Films were deposited on to ITO coated glass substrates (PsiOtec, UK Ltd.), cleaned by sequential washing in acetone, isopropanol and de-ionised water. Atomic force microscopy (AFM) and 4-point probe measurements of the bare substrates yields RMS roughness and sheet resistance values of ~ 3.5 nm and 12 – 15 Ω/sq respectively. Precipitate-free P3HT films were spin-coated at 1500 rpm for 30 s (Merck RR 120 $\text{kg}\cdot\text{mol}^{-1}$, 15 $\text{mg}\cdot\text{ml}^{-1}$ P3HT in chlorobenzene).

ZnO deposition: PLD apparatus and experimental methods are described in detail elsewhere.^[15] Briefly, a KrF laser with wavelength 248 nm was used with a pulse duration of 25 ns. A ZnO target measuring 22 mm diameter was prepared from ZnO powder (Aldrich 99.999 %) pressed and sintered at 1000 °C under flowing oxygen for 10 hours. Laser frequency, target-substrate distance and spot size were fixed for all experiments at 8 Hz, 50 mm and 20 mm^2 respectively. Substrates were held at 200 °C for 15 minutes prior to

deposition. The laser power used was set at 500 mJ leading to a laser power density of 0.82 J.cm^{-2} , for all experiments the number of pulses was fixed at 5000. A background pressure of 3×10^{-5} mtorr was maintained and the oxygen pressure was varied (5, 25, 50, 100, 250 mtorr). Following growth the films were allowed to cool to room temperature. No post-annealing steps were performed.

Electron microscopy: Film morphology and thicknesses were assessed using a LEO Gemini 1525 field emission gun scanning electron microscope (FEG-SEM), operating at 5-10 kV. Cross-sections were prepared using a FEI Helios dual-beam FIB-SEM and subsequent TEM images using a JEOL 2000 FX TEM.

X-ray diffraction measurements: XRD measurements were performed with a PANalytical X'Pert pro MPD diffractometer equipped with an X'celerator detector using Cu K α radiation ($\lambda = 1.5418 \text{ \AA}$), operated at 40 kV and 40mA in conventional reflection mode.

UV-Vis absorption spectroscopy: UV-Vis spectroscopy was carried out using a monochromated white light source (300 – 900 nm) attached to a custom optical bench, controlled by BenWin+ software.

Device performance assessment: Three 150 nm thick silver contacts (1 x 8 mm each) were evaporated on the multilayer structures. Measurements were obtained using a Newport solar simulator with an AM 1.5 output, the current measured during dark and light scans over the range (-0.5 – 0.5 V) were obtained using a Keithley 2400 sourcemeter, all measurements were carried out in air.

Acknowledgements

The authors are grateful to Dr Peter Petrov (Imperial) and Professor David McComb (now at Ohio State University) for useful discussions and technical advice. J.B.F. and J.D. are grateful to the EPSRC for PhD studentships. M.A.M is funded by the Royal Academy of Engineering through a Research Fellowship.

References

- [1] A. J. Said, G. Poize, C. Martini, D. Ferry, W. Marine, S. Giorgio, F. Fages, J. Hocq, J. Bouclé, J. Nelson, J. R. Durrant, J. Ackermann, *The Journal of Physical Chemistry C* **2010**, *114*, 11273.
- [2] P. Atienzar, T. Ishwara, B. N. Illy, M. P. Ryan, B. C. O'Regan, J. R. Durrant, J. Nelson, *The Journal of Physical Chemistry Letters* **2010**, *1*, 708.
- [3] Y.-J. Lee, M. T. Lloyd, D. C. Olson, R. K. Grubbs, P. Lu, R. J. Davis, J. A. Voigt, J. W. P. Hsu, *The Journal of Physical Chemistry C* **2009**, *113*, 15778.
- [4] S. D. Oosterhout, M. M. Wienk, S. S. van Bavel, R. Thiedmann, L. Jan Anton Koster, J. Gilot, J. Loos, V. Schmidt, R. A. J. Janssen, *Nature Materials* **2009**, *8*, 818.
- [5] D. C. Olson, Y.-J. Lee, M. S. White, N. Kopidakis, S. E. Shaheen, D. S. Ginley, J. A. Voigt, J. W. P. Hsu, *The Journal of Physical Chemistry C* **2008**, *112*, 9544.
- [6] L. Baeten, B. Conings, H.-G. Boyen, J. D'Haen, A. Hardy, M. D'Olieslaeger, J. V. Manca, M. K. Van Bael, *Advanced Materials* **2011**, doi: 10.1002/adma.201100414.
- [7] J. Y. Kim, S. H. Kim, H. H. Lee, K. Lee, W. Ma, X. Gong, A. J. Heeger, *Advanced Materials* **2006**, *18*, 572.
- [8] J. Gilot, I. Barbu, M. M. Wienk, R. A. J. Janssen, *Applied Physics Letters* **2007**, *91*, 113520.
- [9] J.-A. Jeong, et al., *Journal of Physics D: Applied Physics* **2010**, *43*, 465403.
- [10] M. Sessolo, H. J. Bolink, *Advanced Materials* **2011**, *23*, 1829.
- [11] N. Bano, S. Zaman, A. Zainelabdin, S. Hussain, I. Hussain, O. Nur, M. Willander, *Journal of Applied Physics* **2010**, *108*, 043103.
- [12] S. Schumann, R. Da Campo, B. Illy, A. C. Cruickshank, M. A. McLachlan, M. P. Ryan, D. J. Riley, D. W. McComb, T. S. Jones, *Journal of Materials Chemistry* **2011**, *21*, 2381.
- [13] J. C. Wang, W. T. Weng, M. Y. Tsai, M. K. Lee, S. F. Horng, T. P. Perng, C. C. Kei, C. C. Yu, H. F. Meng, *Journal of Materials Chemistry* **2010**, *20*, 862.
- [14] J. Gilot, M. M. Wienk, R. A. J. Janssen, *Applied Physics Letters* **2007**, *90*, 143512.
- [15] J. B. Franklin, B. Zou, P. Petrov, D. W. McComb, M. P. Ryan, M. A. McLachlan, *Journal of Materials Chemistry* **2011**, *21* (22), 8178 – 8182.
- [16] H. Kim, J. S. Horwitz, G. P. Kushto, Z. H. Kafafi, D. B. Chrisey, *Applied Physics Letters* **2001**, *79*, 284.
- [17] S. E. Shaheen, C. J. Brabec, N. S. Sariciftci, F. Padinger, T. Fromherz, J. C. Hummelen, *Applied Physics Letters* **2001**, *78*, 841.
- [18] Y. Sahin, S. Alem, R. de Bettignies, J.-M. Nunzi, *Thin Solid Films* **2005**, *476*, 340.
- [19] M. T. Lloyd, D. C. Olson, P. Lu, E. Fang, D. L. Moore, M. S. White, M. O. Reese, D. S. Ginley, J. W. P. Hsu, *Journal of Materials Chemistry* **2009**, *19*, 7638.
- [20] J. Weickert, R. B. Dunbar, H. C. Hesse, W. Wiedemann, L. Schmidt-Mende, *Advanced Materials* **2011**, *23*, 1810.
- [21] F. Claeysens, A. Cheesman, S. J. Henley, M. N. R. Ashfold, *Journal of Applied Physics* **2002**, *92*, 6886.
- [22] K. Ellmer, A. Klein, B. Rech, *Transparent Conductive Zinc Oxide Basics and Applications in Thin Film Solar Cells*, Vol. 104, Springer, **2008**.

- [23] T. Nobis, E. M. Kaidashev, A. Rahm, M. Lorenz, M. Grundmann, *Physical Review Letters* **2004**, *93*, 103903.
- [24] C.-H. Wu, H. Li, H. H. Fong, V. A. Pozdin, L. A. Estroff, G. G. Malliaras, *Organic Electronics* **2011**, *12*, 1073.
- [25] V. Shrotriya, J. Ouyang, R. J. Tseng, G. Li, Y. Yang, *Chemical Physics Letters* **2005**, *411*, 138.
- [26] M. S. White, D. C. Olson, N. Kopidakis, A. M. Nardes, D. S. Ginley, J. J. Berry, *Physica Status Solidi (a)* **2010**, *207*, 1257.

Figure 1 a) A typical XRD pattern for ZnO film deposited at 200 °C, 50 mtorr, showing characteristic (002) ZnO peaks and substrate peaks, b) shows the observed change in peak position and intensity with oxygen pressure (5-250 mtorr).

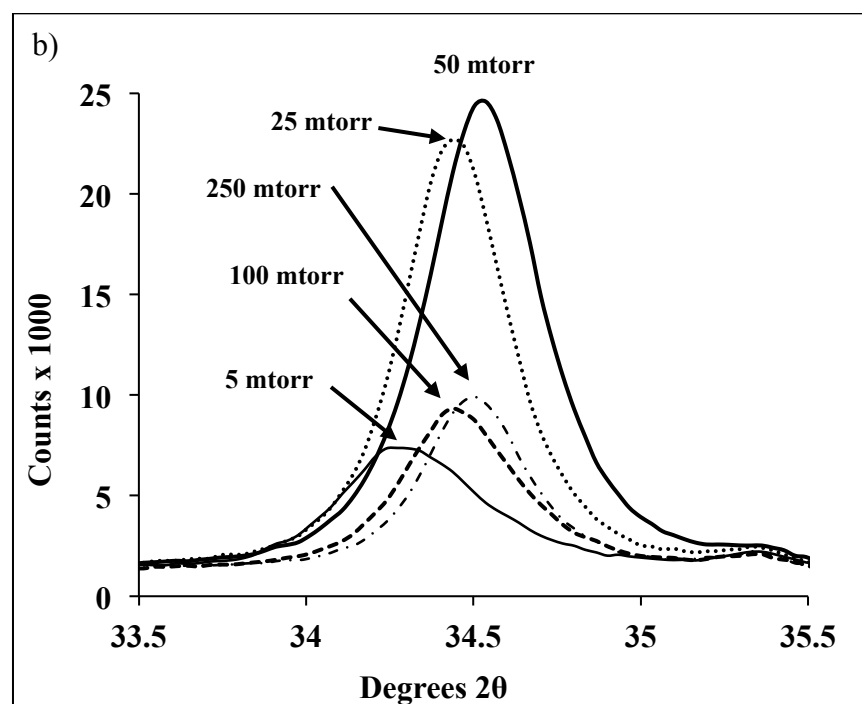
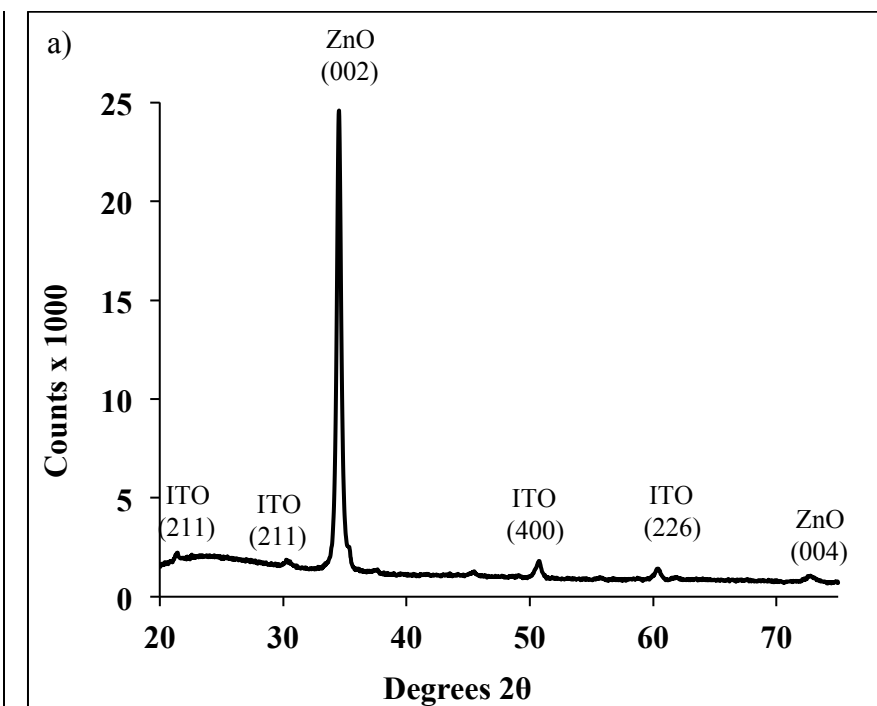


Figure 2 SEM micrographs showing surface the morphology of films deposited at a background oxygen pressure of; a) 5 mtorr, b) 250 mtorr, c) 50 mtorr. TEM micrographs showing d) individual layers of a multilayer conventional architecture h-PV device and e) detailed view of P3HT/ZnO interface showing no visible damage layer. Note that the Au and Pt layers were deposited for FIB imaging and sample preparation.

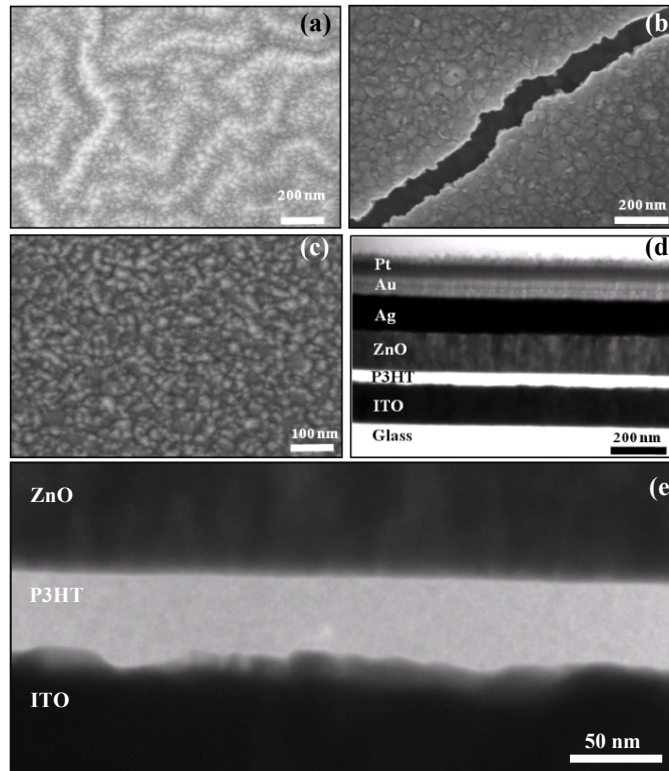


Figure 3 a) shows UV-vis transmission spectra for ITO/P3HT, ITO/P3HT/ZnO and ITO/ZnO/P3HT films (ZnO deposited at 50 mtorr, 200 °C), b) J-V data for ITO/P3HT/ZnO/Ag device shown in figure 2d-e).

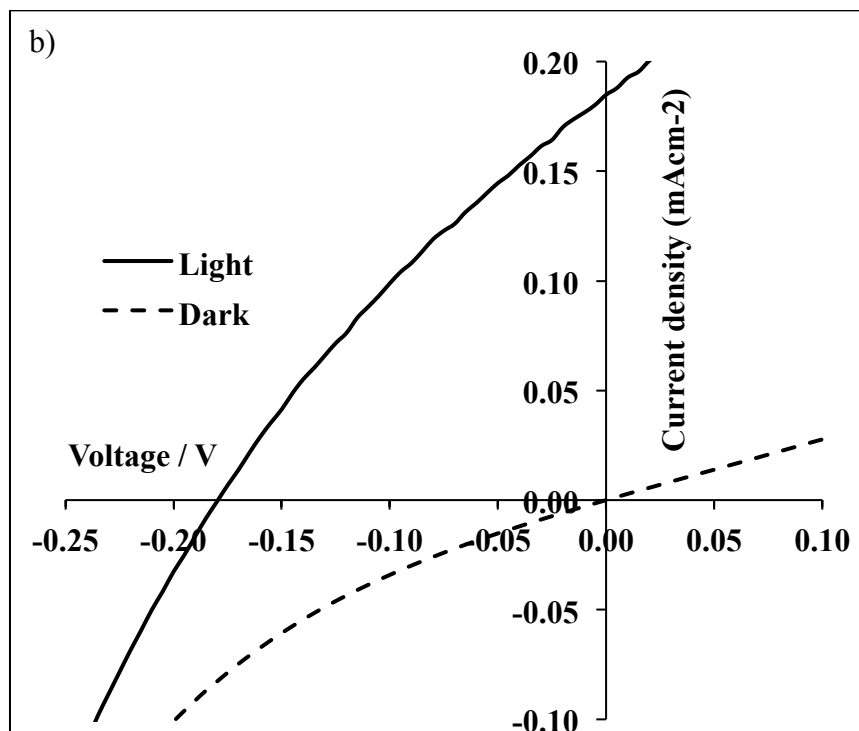
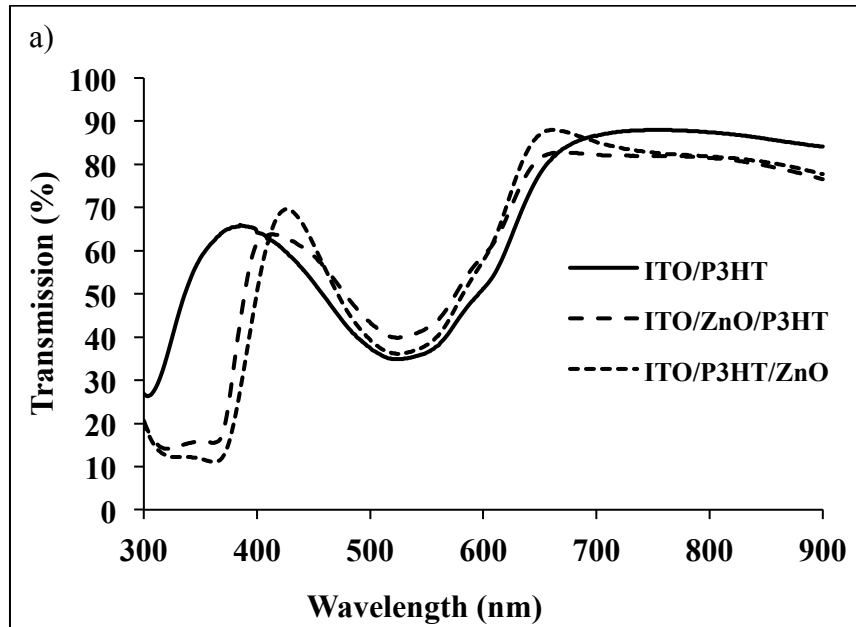


Table 1 Peak position, full width at half-maximum (FWHM), thickness and grain size calculated by the Scherrer method of the ZnO film, extracted from the XRD data in Figure 1

Oxygen pressure (mtorr)	(002) peak position $^{\circ}2\theta$	FWHM $^{\circ}2\theta$	Film thickness (nm)	Grain size (nm)
5	34.30	0.47	160	213 \pm 3
25	34.44	0.37	166	287 \pm 5
50	34.53	0.40	170	260 \pm 4
100	34.57	0.38	124	277 \pm 5
250	34.50	0.35	128	308 \pm 6

ToC entry

The deposition of highly crystalline ZnO onto P3HT using pulsed laser deposition at low temperature is discussed. To demonstrate the applicability of the technique we outline for the first time the preparation of a conventional architecture hybrid photovoltaic device. No degradation of the microstructure, optical or electronic properties of the P3HT were observed. The methodology is widely applicable for depositing oxide interlayers and optical spacers in multilayer organic devices.

Keyword: Zinc Oxide, Conjugated Polymers, Organic Electronics, Thin Films, Hybrid Materials

*Joseph B. Franklin, Jonathan Downing, Finn Giuliani, Mary P. Ryan and Martyn A. McLachlan**

Building on Soft Foundations – New Possibilities for Controlling Hybrid Photovoltaic Architectures

ToC figure

